Proceedings of the XVII ECSMGE-2019
Geotechnical Engineering foundation of the future
ISBN 978-9935-9436-1-3

doi: 10.32075/17ECSMGE-2019-0870

XVII European Conference
ECSMGE 2019
Reykjavik
on Soil Mechanics
and Geotechnical Engineering

Application of associated or non-associated flow rule to typical failure problem

Application de la règle de flux associée ou non associée à un problème de défaillance typique

N. Mortensen
nmGeo, Allerød, Denmark

A. Krogsbøll
nmGeo, Allerød, Denmark (former)

ABSTRACT: General types of failure problems are analysed and compared using Finite Element Modelling, limit analyses and analytical solutions to indicate the effect of superposition and applying non-associated flow rule and the effect of introducing a modified friction angle. It is shown that the modified friction angle is a safe approach, and suited for passive earth pressure, but it overestimates the effect of non-associated flow for bearing capacity and active earth pressure. The safety approach as defined by a reduction of the friction angle is discussed and proved to be compromised in some cases.

RÉSUMÉ: Les types généraux de problèmes de défaillance sont analysés et comparés à l'aide de la modélisation par éléments finis, d'analyses limites et de solutions analytiques afin d'indiquer l'effet de la superposition et de l'application de la règle de flux non associée, ainsi que de l'introduction d'un angle de frottement modifié. Il est démontré que l'angle de frottement modifié est une approche sûre et convient à la pression de terre passive, mais il surestime l'effet de l'écoulement non associé sur la capacité portante et la pression de terre active. L'approche de sécurité définie par une réduction de l'angle de frottement est discutée et s'est avérée compromise dans certains cas.

Keywords: Flow rule; Dilation angle; Ultimate limit state; Accuracy of parameters

1 INTRODUCTION

Typical failure problems like the bearing capacity of footings, the total earth pressure on a wall or a slope stability are often solved using methods involving a series of simplifications. The ground model is a simplified geometry with layers of homogeneous properties defined by constitutive models. The constitutive models are simplifications of the soil behaviour. The methods applied for analysis may represent approximations to the physics governing the problem in question. Effort should therefore be put into the important part of a problem more than to minor details. Engineers should ensure a consistent balance between assumptions and the problem in question. Vaughan (1994) stressed the importance of controlling theory against practice, as Terzaghi and Peck (1948) did before that. Vaughan (1994) also made the point that sophisticated models should not be applied on everyday problems, when experience and standard techniques for years were adequate, and proved no problems. Potts (2003) discussed application of numerical analyses to geotechnical problems and highlighted that numerical analyses

may provide more reliable solutions and cost savings.

The objective of this paper is to discuss the degree of certainty by which the ultimate limit state can be addressed considering the simplest cases in geotechnical engineering assuming a drained Mohr Coulomb state.

2 PRINCIPAL CONSIDERATIONS

The upper and lower bound theorem showed that a statically admissible solution is either exact or on the safe side whereas a kinematically admissible solution is either exact or on the unsafe side. These conclusions assumed associated flow, i.e. dilation angle ψ is equal to friction angle φ'.

Laboratory testing of a soil in a drained state shows that $\psi < \varphi'$ (non-associated flow), which means that the upper and lower bound theorem is no longer valid, and that statically admissible solution therefore may be on the unsafe side.

A series of closed form expressions are available for estimation of bearing capacity factors and earth pressure coefficients, when accepting associated flow. Otherwise, the use of numerical modelling is required. In this paper the non-associated flow is investigated using the finite element method.

3 ANALYSED CASES

The bearing capacity of a footing and the earth pressure on a vertical wall were used for the evaluation of effect of non-associated flow.

3.1 Bearing capacity case

Figure 1 illustrates a 2D bearing capacity case for a coarse grained soil with an effective unit weight *γ'* and a peak friction angle of *φ'* loaded by a surcharge *q'*.

A plastic failure is developed when the load *R* (kN/m) exceeds the capacity of the soil. The analytical bearing capacity formula is given by equation (1).

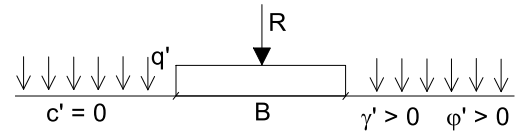

Figure 1. Bearing capacity of a strip footing.

$$b = \frac{R}{B} = \mu_1 \left(\tfrac{1}{2} \cdot \gamma' \cdot N_\gamma \cdot B + q' \cdot N_q\right) \qquad (1)$$

Where the bearing capacity factors N_γ and N_q are given in Equation (2) and where μ_1 is a scaling factor. N_γ was solved by Lundgren & Mortensen (1953) while N_q was established by Prandtl (1920). The approximate expression for N_γ in Equation (2) is adopted from DS/EN 1997-1 DK NA.

$$N_\gamma = \tfrac{1}{4}\left(\left[N_q - 1\right] cos\, \varphi'\right)^{3/2}$$
$$N_q = \frac{1 + sin\, \varphi'}{1 - sin\, \varphi'} e^{\pi\, tan\, \varphi'} \qquad (2)$$

The values applied for N_γ in this paper are based on the approach suggested by Lundgren & Mortensen (1953) and not by the approximation in Equation (2). Results from Equation (1) were compared with results from the finite element program Plaxis 2D with 15-noded elements. The effect of associated flow and non-associated flow was studied for cases where non-associated flow was defined by Equation (3).

$$\psi = max(\varphi' - 30°; 0) \qquad (3)$$

Estimates were conducted for friction angles between 26° and 38° using γ' = 10 kN/m^3, a foundation width B of 3.0 m and a surcharge of 15 kPa. Failure in the soil was introduced by prescribed vertical displacements of the foundation.

The number of elements in Plaxis 2D was decided based on the criterion that the numerical solution assuming associated flow and γ' = 0 for φ'

= 38° were calculated within 1% accuracy relative to the Prandtl case, and the same element net was then used for all the analyses.

3.2 Earth pressure case

A vertical and fully rough wall retains a coarse grained soil with a horizontal soil surface loaded by a sucharge load, *q'*. The wall rotates around the tip until a passive pressure is achieved. The total earth pressure, *E* acting on the wall is defined by:

$$E = \mu_2\left(\tfrac{1}{2}\cdot\gamma'\cdot H^2\cdot K_\gamma^p + q'\cdot K_q^p\cdot H\right) \qquad (4)$$

Where μ_2 is a scaling factor, *H* is the height of the wall and where the passive earth pressure coefficients K_γ^p and K_q^p are given by:

$$K_\gamma^p = K_q^p / \cos\varphi'$$
$$K_q^p = (1+\sin\varphi')\cdot e^{\left(\frac{\pi}{2}+\varphi'\right)\tan\varphi'} \qquad (5)$$

The passive earth pressure coefficient for the γ'-case in Equation (5) is an approximation to the solution used in the present paper, which is also discussed in Mortensen & Krogsbøll (2019). The coefficient from the q-case is from Prandtl (1920). For active earth pressure the coefficient for the *q'*-case is used for the *q'*-case as well as the γ'-case. It is derived from the same formulas (5) with negative friction angle.

The parameter variation followed that of the bearing capacity case except that the 3.0 m foundation width is replaced by a fully rough vertical wall with a height of 3.0 m.

4 MATERIAL MODELS

The soil model applied is based on linear elastic, perfectly plastic soil behaviour following Mohr-Coulombs failure criterion.

Deformation properties were Young's modulus $E = 200$ MPa, Poisson's ratio $\nu = 0.3$.

A way to account for non-associated flow is to apply a method based on associated flow, but introducing a modified friction angle φ'_{mod}:

$$\tan\varphi'_{mod} = \frac{\sin\varphi'\cos\psi}{1-\sin\varphi'\sin\psi} \qquad (6)$$

This principle has been described by e.g. Davis (1968). Equation (6) was analysed too.

5 RESULTS AND DISCUSSION

5.1 Bearing capacity

Table 1 gives the bearing capacity factors N_γ and N_q for selected values of φ' together with the estimated bearing capacity from Equation (1) setting $\mu_1 = 1.0$.

Table 1. Bearing capacity factors and the bearing capacity, b, from Equation (1) setting $\mu_1 = 1.0$.

φ´	N_γ	N_q	b [kPa]
26°	7.64	11.9	292
28°	10.6	14.7	380
30°	14.8	18.4	497
34°	29.0	29.4	876
38°	58.9	48.9	1,618

Table 2 shows the corresponding bearing capacities from Plaxis 2D using associated flow (AF) and non-associated flow (NAF) according to Equation (3).

Table 2. Bearing capacities, b, from Plaxis 2D with associated flow (AF) and non-associated flow (NAF).

φ´	b^{AF} [kPa]	φ'^{AF}_{rep}	b^{NAF} [kPa]	φ'^{NAF}_{rep}
26°	361	27.6°	315	26.6°
28°	468	29.6°	393	28.3°
30°	611	31.5°	490	29.9°
34°	1,071	35.4°	818	33.6°
38°	1,970	39.3°	1,387	37.1°

The friction angles, φ'^{AF}_{rep} and φ'^{NAF}_{rep} in Table 2 represent the friction angles required when using

Equation (1) to back-calculate b^{AF} and b^{NAF}, respectively, setting the scaling factor $\mu_1 = 1.0$. The bearing capacities calculated with Plaxis 2D and associated flow (Table 2) are higher than the capacities in Table 1 based on Equation (1). This difference owes to the fact that the bearing capacity factor N_q is derived assuming $\gamma' = 0$ and N_γ is derived for $q' = 0$. The individual bearing capacity factors therefore refer to failure mechanisms without coupling, while the scaling factor, μ_1, models the combined effect when γ' and q' are applied within one failure mechanism. The coupled solution may be solved by different techniques and Figure 2 shows the value of μ_1 as found by the approach suggested by Martin (2004) combined with Equation (1).

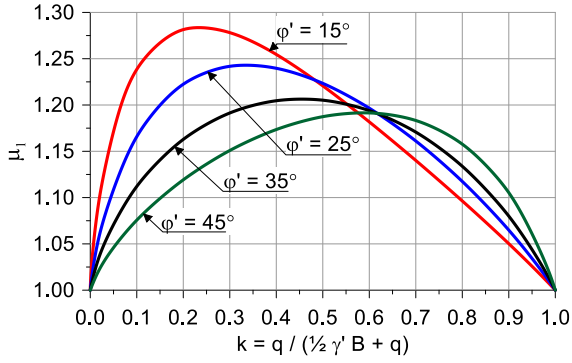

Figure 2. Scaling factor, μ_1, from Equation (1) against the ratio, k, introduced to normalise the combined effect of q', γ', and B for various friction angles.

In the pure γ'-case, k on the x-axis of Figure 2 is zero, and in the pure surcharge case k is 1. In both cases $\mu_1 = 1$. For values of k between 0 and 1 the coupled effect of γ and q' is illustrated in terms of the scaling factor μ_1 to be applied in Equation (1).

Figure 3 shows the bearing capacities for associated flow b^{AF} from Table 2 (includes the coupling effect between γ' and q'), normalised with the bearing capacities, b, from Table 1 (setting $\mu_1 = 1.0$). In addition, Figure 3 also illustrates the value of μ_1 from Figure 2.

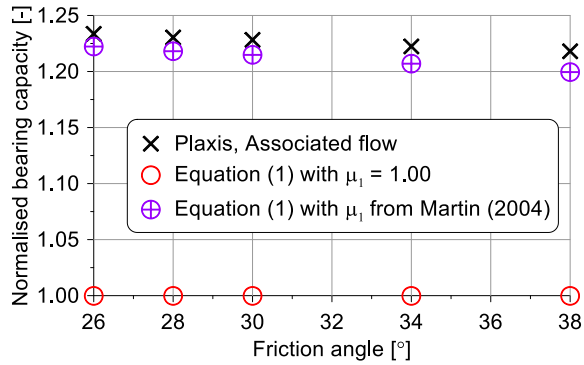

Figure 3. Effect of coupling compared to superposition. The normalised bearing capacity (Plaxis) for associated flow b^{AF}/b, with $\mu_1 = 1.0$. Results including μ_1 from Figure 2 are also included.

Figure 3 illustrates that Plaxis 2D will overshoot the estimated bearing capacity from Equation (1) by approximately 22-23 %. The estimates in this section reflects k = 0.50 (x-axis on Figure 2), so the overshoot is not constant but just a result of the properties applied (γ'=10 kN/m^3, B=3 m and q'=15 kPa).

The load-displacement curve from Plaxis 2D differs when comparing associated flow with non-associated flow, cf. Figure 4. The bearing capacity is uniquely defined for associated flow exhibiting a plastic roof, whereas the typical picture for non-associated flow is a peak value followed by an oscillating curve caused by bifurcation.

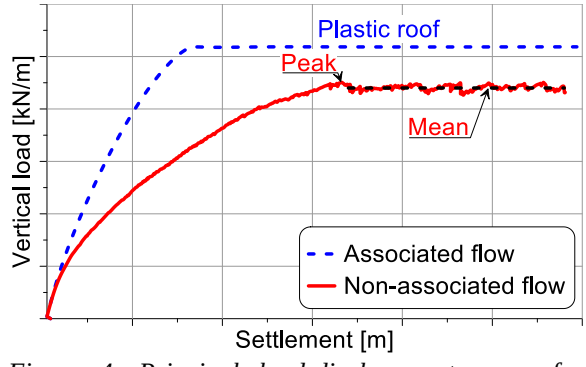

Figure 4. Principal load-displacement curve for associated and non-associated analyses.

If both the peak value and the mean value from Figure 4 are back-calculated to friction angles using Equation (1), the difference between these friction angles is typically 0.4°-0.6°. Analysis with non-associated flow in this paper is for simplicity represented by the peak value.

Figure 5 shows the bearing capacities b^{NAF} from non-associated flow in Table 2 normalised with the bearing capacities b in Table 1 ($\mu_1 = 1.0$).

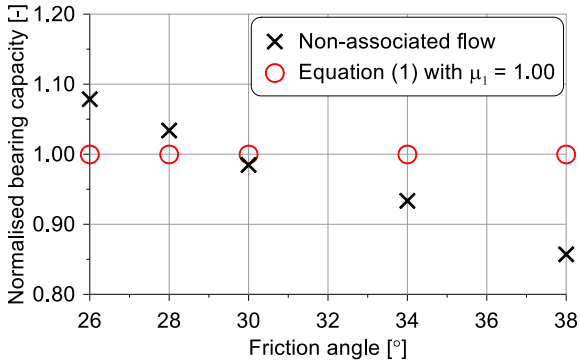

Figure 5. The normalised Plaxis 2D bearing capacity b^{NAF}/b for non-associated flow, with $\mu_1 = 1.0$.

It is seen from Table 2 and Figures 3 and 5 that capacities from Plaxis with associated flow are expectedly higher than those from non-associated flow. Figure 5 shows that the combination of φ' = 30° and ψ = 0° implies an almost identical bearing capacity as Equation (1) with $\mu_1 = 1.0$. For friction angles lower than 30°, the non-associated capacities are higher than found by Equation (1). Non-associated flow tends to reduce the capacity while coupling effects between q' and γ' tends to increase the capacity. As the friction angle increases in Figure 5, the negative effect from non-associated flow seems to take over relative to the positive effect from coupling.

5.2 Passive earth pressures

Table 3 gives the passive earth pressure coefficients from Equation (5) for selected values of φ' together with the estimated total earth pressure from Equation (4) setting the scaling factor $\mu_2 = 1.0$.

Table 3. Passive earth pressure coefficients from Equation (5) and the total passive earth pressure from Equation (4) setting $\mu_2 = 1.0$.

φ´	K_γ^p	K_q^p	E [kN/m]
26°	4.23	3.86	367
28°	4.88	4.39	417
30°	5.67	5.03	481
34°	7.85	6.71	656
38°	11.3	9.25	927

Table 4 shows the estimated total passive earth pressures from Plaxis 2D using associated and non-associated flow and applying Equation (3) for non-associated flow.

Table 4. The total passive earth pressure estimated by Plaxis 2D with associated flow (AF) and non-associated flow (NAF).

φ´	E^{AF} [kN/m]	φ'^{AF}_{rep}	E^{NAF} [kN/m]	φ'^{NAF}_{rep}
26°	375	26.5°	333	24.6°
28°	431	28.5°	365	26.1°
30°	500	30.5°	399	27.3°
34°	686	34.5°	521	31.1°
38°	978	38.6°	691	34.7°

The friction angles, φ'^{AF}_{rep} and φ'^{NAF}_{rep} in Table 4 represent the friction angles required when using Equation (4) to back-calculate E^{AF} and E^{NAF}, respectively, with the scaling factor $\mu_2 = 1.0$.

Figure 6 shows the earth pressures from Table 4 normalised with the earth pressure from Table 3. The effect of linear super position for associated flow can be seen from Figure 3 (bearing capacity) and Figure 6 (earth pressure). It is seen that the effect is less pronounced for passive earth pressures (3-6%) than for bearing capacity (20-22 %). The conclusion is that bearing capacity following Equation (1) is less accurate relative to the earth pressure following Equation (4) when associated flow is considered, and scaling factors of unity are used.

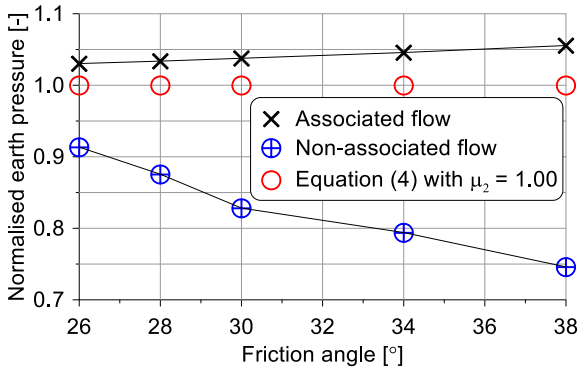

Figure 6. The normalised total passive earth pressure from Table 4 E^{AF}/E for associated and E^{NAF}/E for non-associated flow.

Non-associated flow will, however, not impact the estimated bearing capacity in Figure 5 to the same degree as seen for passive earth pressures in Figure 6 but this is due to coupling effects rather than to $\psi < \varphi$'.

5.3 Active earth pressures

Figure 6 is based on passive earth pressures while Figure 7 together with the Tables 5 and 6 represents active earth pressures. As Plaxis is a kinematically admissible solution, the result will always be on the unsafe side, so the active earth pressure is estimated too low and the normalised earth pressure for associated flow in Figure 7 is thus lower than 1.0 while the corresponding non-associated results are higher than 1.0.

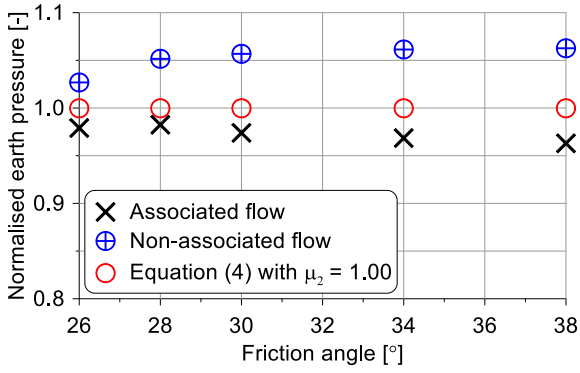

Figure 7. The normalised total active earth pressure for associated and non-associated flow, normalised with Equation (4) (active version) setting $\mu_2 = 1.0$.

Table 5. Active earth pressure coefficients and the total active earth pressure using Equation (4) setting $\mu_2 = 1.0$.

φ'	K_γ^a	K_q^a	E [kN/m]
26°	0.318	0.326	29.0
28°	0.291	0.295	26.4
30°	0.266	0.273	24.3
34°	0.222	0.228	20.2
38°	0.184	0.189	16.8

Table 6. The total active earth pressure estimated by Plaxis 2D with associated flow (AF) and non-associated flow (NAF).

φ'	E^{AF} [kN/m]	φ'^{AF}_{rep}	E^{NAF} [kN/m]	φ'^{NAF}_{rep}
26°	28.4	26.5°	29.7	25.4°
28°	25.9	28.5°	27.7	27.0°
30°	23.6	30.6°	25.7	28.8°
34°	19.6	34.7°	21.5	32.7°
38°	16.2	38.8°	17.8	36.7°

Figure 7 shows that the effect of coupling for an active case is of the same magnitude as that of a passive case, while the effect of non-associated flow is limited; 6 % for $\varphi' = 38°$ in the active case while 25 % is observed for the corresponding passive case in Figure 6.

6 OVERALL DISCUSSION

An exact estimate of a bearing capacity or a total earth pressure will rely on mainly three different but correlated aspects: a) The type of structure, b) the representative friction angle and c) dilation.

The term "representative" friction angle means that the analysis assumes one value of φ' to cover the entire failure mechanism. The effective mean stress within a bearing capacity mechanism may vary by a factor of 10 or even more and the corresponding φ' may therefore change by up to 10-12°. For an active earth pressure, the effective mean stress is significantly smaller, and the change of effective mean stress level is rather modest - and so is the variation in φ' throughout

the mechanism. It is therefore decisive that e.g. the type of structure and the effective mean stress level is included when identifying a representative friction angle for the project in question. The above given considerations have not been debated further within this paper.

Results presented in this paper indicate that if a simple bearing capacity formula in line with Equation (1) is used as a basis for comparison, a variation of ±1° in the friction angle will typically account for likely variations in the angle of dilation provided that the combined effect of γ', q' and the foundation width plots within the interval of 0.25 to 0.75 of the x-axis on Figure 2. Outside this range of 0.25 to 0.75, that is in cases dominated by one of the components γ' or q', the effect of dilation will change.

The rather narrow range in φ' indicates that the bearing capacity formula is suited for its purpose, but this is questionable. The narrow range reflects that linear superposition adds an unused safety margin to the analysis, which is counteracted by the effect of non-associated flow.

The tendencies for passive earth pressures are somehow different. The closed-form expressions from Equation (4) will tend to over predict the resistance in a soil following non-associated flow. Table 4 shows $\varphi'^{AF}_{rep} = 38.6°$ and $\varphi'^{NAF}_{rep} = 34.7°$ for $\varphi' = 38°$. The upper value of 38.6° is close to the input value of 38.0°, which indicates that superposition is less pronounced for passive pressures. The low value of 34.7° indicates that the effect of non-associated flow is high. Assuming a partial factor of 1.20 to be applied on $\tan\varphi'$ with a characteristic value 38.0°, implies a design value of 33.1° which is not much lower than the representative characteristic value of 34.7°. Care should therefore be taken when establishing representative friction angles for passive earth pressures, because the safety will be influenced.

For the passive case discussed above with a representative friction angle varying between 34.7° and 38.6° the similar range for an active earth pressure narrows down to 36.7° - 38.8°. The difference is only half of that seen for the passive case and active earth pressures are thus less sensitive to the effect of non-associated flow.

The modified friction angle in Equation (6) transforms φ' for non-associated flow to a lower friction angle, φ'_{mod} to be used for associated flow. The difference $\Delta\varphi' = \varphi' - \varphi'_{mod}$ is shown in Figure 8 as a function of φ'.

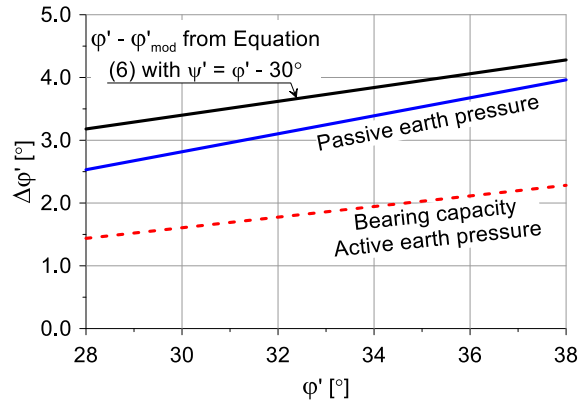

Figure 8. The value of $\Delta\varphi'$ against the friction angle φ'.

The other curves in Figure 8 show how much the friction angle must be reduced ($\Delta\varphi$) in order to get a safe approach, if the capacity or earth pressure is found assuming associated flow as compared to applying non-associated flow. Data from Table 4 has been used in the following way: a) Establish a function $E^{AF}(\varphi')$ where the passive pressure for associated flow is expressed as a function of φ' through a third order polynomial; b) Solve the equation $E^{AF}(\varphi'_1) = E^{NAF}$; c) Define $\Delta\varphi' = \varphi' - \varphi'_1$. The y-axis in Figure 8 shows $\Delta\varphi'$ while the x-axis represents the value φ' for non-associated flow, and Equation (6) can thus be evaluated.

Figure 8 shows that Equation (6) is a safe approach, leading to reasonable estimates for passive pressures. The curve in Figure 8 for bearing capacity and active earth pressure has been established by the same approach, using data from Table 2 and 6, respectively. The two different cases end up at almost the same result and are presented by a single curve. The correction required ($\Delta\varphi'$)

for active pressure and bearing capacity, and thus the effect of accounting for non-associated flow, is smaller than for passive pressures, and the approximation from Equation (6) seems to overestimate that effect.

7 CONCLUSIONS

The conclusions presented in this paper concern the ultimate limit state:

The most important single factor in the analysis of failure problems in frictional materials is the friction angle. Effort should therefore be put into determination of this decisive parameter if a safety analysis should be improved and safety guaranteed. The precision of the dilation angle is not important, but it is important whether associated or non-associated flow is considered and this choice will influence the friction angle applied.

The safety of a failure problem is not uniquely defined, when safety is accounted for by using partial coefficient to the characteristic value of $\tan\varphi$. This principle will lead to low safety for low frictional angles and vice versa. For low friction angles the effect of superposition is significant, and therefore the factual safety will be increased. For high friction angles the effect of non-associated flow will be significant, and factual safety will be decreased: A closed form expression for bearing capacity, not accounting for non-associated flow, will result in overestimation of capacities for high friction angles. For lower friction angles the effects of superposition and non-associated flow counteracts each other.

For passive earth pressures it is necessary to account for non-associated flow, otherwise the capacity is significantly overestimated. The approximation introduced by the modified frictional, φ'_{mod}, is a safe approach.

The uncertainty of the safety factor to a failure problem indicated by choosing different solution techniques, is of the same magnitude as the effect of changing the friction angle by approximately ±2°. Therefore, the safety factor is not uniquely defined, and it makes no sense to optimize a structure to a safety factor determined with a high accuracy.

The frictional angle representing a failure problem must be defined according to the failure problem in question and the methods applied for verification of the safety.

8 ACKNOWLEDGEMENTS

The authors are very grateful for the financial support provided by the company nmGeo, which made it possible to present this paper.

9 REFERENCES

Davis, E.H. 1968. Theories of plasticity and failure of soil masses. In: *Soil Mechanics, selected topics*, ed. I.K. Lee, Butterworths, London. p341-381.

Lundgren, H. & Mortensen, K. 1953. Determination of the Theory of Plasticity of the Bearing Capacity of Continuous Footings on Sand. *Proccedings 3rd Int. Conf. Soil Mech. & Found. Eng*. Vol 1, p 409-412, Zürich.

Martin, C.M. 2004. User's Guide. ABC – Analysis of Bearing Capacity, Version 1.0. Department of Engineering Science, University of Oxford, OUEL Report No. 2261/03.

Mortensen, N., Krogsbøll, A. 2019. Effect of tangential surface load components on earth pressure coefficients. *Proc. XVII ECSMGE-2019, Iceland*.

Potts, D.M. 2003. Numerical analysis: a virtual dream or practical reality? *Géotechnique* **53**, No 6, 535-573.

Prandtl, L. 1920. Über die Harte Platischer Korper. *Nach Gesell. Wiss. Göttingen, Math-Phys. KL*, pp74ff.

Terzaghi, K. Peck, P.B. 1948. *Soil Mechanics in engineering practice*, 1st edn., Wiley, New York.

Vaughan, P.R. 1994. Assumption, prediction and reality in geotechnical engineering, *Géotechnique* **44**, No 4, 573-609.